2926–2935 *Nucleic Acids Research, 2016, Vol. 44, No. 6* *Published online 13 January 2016*
doi: 10.1093/nar/gkw003

The exception that confirms the rule: a higher-order telomeric G-quadruplex structure more stable in sodium than in potassium

Carole Saintomé[1,2], Samir Amrane[3,4], Jean-Louis Mergny[3,4] and Patrizia Alberti[1,*]

[1]Structure et Instabilité des Génomes, Sorbonne Universités, Muséum national d'Histoire naturelle, Inserm U 1154, CNRS UMR 7196, Paris, France, [2]UPMC (Université Pierre et Marie Curie) Université Paris 6, UFR 927, Paris, France, [3]Université de Bordeaux, ARNA Laboratory, Bordeaux, France and [4]IECB (Institut Européen de Chimie et Biologie), Inserm U 869, Pessac, France

Received September 22, 2015; Revised December 29, 2015; Accepted December 31, 2015

ABSTRACT

DNA and RNA guanine-quadruplexes (G4s) are stabilized by several cations, in particular by potassium and sodium ions. Generally, potassium stabilizes guanine-quartet assemblies to a larger extent than sodium; in this article we report about a higher-order G4 structure more stable in sodium than in potassium. Repeats of the DNA GGGTTA telomeric motif fold into contiguous G4 units. Using three independent approaches (thermal denaturation experiments, isothermal molecular-beacon and protein-binding assays), we show that the $(GGGTTA)_7GGG$ sequence, folding into two contiguous G4 units, exhibits an unusual feature among G4 motifs: despite a lower thermal stability, its sodium conformation is more stable than its potassium counterpart at physiological temperature. Using differential scanning calorimetry and mutated sequences, we show that this switch in the relative stability of the sodium and potassium conformations (occurring around 45°C in 100 mM cation concentration) is the result of a more favorable enthalpy change upon folding in sodium, generated by stabilizing interactions between the two G4 units in the sodium conformation. Our work demonstrates that interactions between G4 structural domains can make a higher-order structure more stable in sodium than in potassium, even though its G4 structural domains are individually more stable in potassium than in sodium.

INTRODUCTION

Cations play an essential role in nucleic acid folding. Among DNA and RNA structures, the stability and the conformation of guanine quadruplexes (G4s) are especially sensitive to the nature of the cation present in solution. The reason of this cation sensitivity was elucidated many years after the first experimental evidence. More than 50 years ago, X-ray diffraction patterns of fibers from guanosine monophosphate gels clearly revealed 'a helical structure with four units per turn of the helix' and a model of cyclic arrangement of four hydrogen-bonded guanines was proposed (1). This arrangement, later named 'G-quartet' (2), had already been considered, a few years before, by Alexander Rich to interpret the X-ray diffraction pattern of polyinosinic acid fibers (3). Nevertheless, at that time, Rich rejected this model in favor of a three-stranded model, because, as he correctly inferred, for the four-stranded structure 'there is a hole in the center … If it is unfilled, it introduces considerable instability' (3). It was later observed that the melting temperature of guanosine gels depended on the nature of the cation present in solution in an anomalous way compared to (double-stranded) DNA: the melting temperature of the gels as a function of the ionic radius of several monovalent cations was a bell-like curve with a maximum corresponding to the potassium ion (4). Only years later, it became clear that the central hole of G-quartets was the key factor of this 'cation anomaly': it was first proposed and later demonstrated that alkali metal ions such as Na^+ and K^+ coordinate to G-quartet assemblies along the central cavity (5–8). The peculiar sensitivity of G-quartet assemblies to the nature of the cation results from the specific coordination of several monovalent or divalent cations by the carbonyl oxygens of the guanines assembled in the tetrad arrangement. In order to be specifically bound by tetrads of guanines, a cation must be small enough to fit in the electron-rich cavity and large enough to bridge the guanine carbonyl oxygens. Monovalent cations stabilize G-quartet assemblies according to the following ranking: $K^+ > Na^+, NH_4^+, Rb^+ >> Li^+, Cs^+$ (4–6,9). Li^+ is too small to bind tightly in the center; Na^+ can fit in a tetrad plane; the larger K^+ can lie in-between two tetrads; Cs^+ is too large to be sandwiched between tetrads at a distance that would still permit tetrad

*To whom correspondence should be addressed. Tel: +33 1 40 79 37 27; Fax: +33 1 40 79 37 05; Email: alberti@mnhn.fr

interactions, as first argued by Pinnavaia *et al*. (5). Preferential binding of K^+ to G4s with respect to Na^+ would be due to a greater energetic cost of Na^+ dehydration (10). Over the years, many studies have explored the role of cations in determining the conformation and the stability of G4 structures and their dynamics in the central cavity (11,12).

So far, G4-prone nucleic acid sequences that have been studied both in sodium and in potassium have displayed higher structural stability in potassium, with very few exceptions. This feature has been reported for non-modified oligonucleotides as well as for chemically-modified oligonucleotides, for intramolecular G4s as well as intermolecular G4s (6,9,13–29). The extent of the difference in stability between the folded form in potassium and the folded form in sodium depends on the sequence; differences in melting temperatures ranging from 1°C to 40°C have been observed (25). For example, among intramolecular DNA G4s, the thrombin binding aptamer displays one of the larger differences in thermal stability between the potassium and the sodium forms (13). Ohtsuka *et al*. took advantage of this large difference in stability to design a fluorescent probe based on the thrombin binding aptamer to image potassium ions in living cells (30). Some sequences display an even more drastic discrimination between K^+ and Na^+ ions, folding into G4s in potassium but not in sodium (P. A. unpublished results). A few exceptions to the $K^+ > Na^+$ general trend for G4 stabilization have been reported. These observations were done on variants of the human telomeric sequence $(GGGTTA)_3GGG$ bearing modifications that affected the ion/tetrad coordination or altered the tetrad composition (substitution of guanines with O6-methylguanines (31), abasic sites (32) or adenine bases (33)). Some of these modifications have been reported to destabilize the natural potassium conformation(s) of the human telomeric G4 to a larger extent than its sodium conformation(s). An apparently higher melting temperature in sodium than in potassium can also result from the equilibrium between a G4 and a non-G4 structure (such as a hairpin), as reported for insect and nematode telomeric sequences ($(GGTTA)_3GG$ and $(GGCTTA)_3GG$, respectively) (26).

In this article we report the first example of a higher-order G4 structure whose sodium conformation is more stable than its potassium conformation. To our knowledge, it is the first example of a G4 structure formed by tetrads of non-modified guanines exhibiting such a feature. DNA long telomeric sequences of the type $(GGGTTA)_{4m-1}GGG$, where $m = 2, 3, 4, \ldots$, fold into high-ordered structures composed of m contiguous G4 units (34–37). In the present article we show that, among these sequences, the $(GGGTTA)_7GGG$ sequence, folding into two contiguous G4s, displays an unusual behavior among G4 motifs, never reported before: despite a lower thermal stability, its sodium conformation is more stable than its potassium counterpart below a threshold temperature (45°C in 100 mM cation concentration). We provide an explication of this behavior in terms of enthalpically favorable interactions between the two G4 units composing the higher-order G4 structure formed by this sequence in sodium. Results on $(GGGTTA)_7GGG$ sequence are presented in the context of long telomeric sequences in sodium. This work also illustrates how misleading melting temperature values can be when considering the physiologically relevant parameters: thermodynamic stability and kinetic parameters at 37°C.

MATERIALS AND METHODS

Oligonucleotides

Oligonucleotides were purchased from Eurogentec (Belgium). They were purified by the manufacturer according to the following protocols: H21, H45, H69 and H93 oligonucleotides used for ultraviolet (UV) absorption measurements, molecular-beacon and protein-binding assays were PAGE purified; the molecular beacon MB was Reverse-Phase HPLC purified; H45 oligonucleotide used for differential scanning calorimetry (DSC), TTA-H45-TTA, H21-$(TTA)_{2,3}$-H21 and H21-$(TTA)_{2,3}$-H21-$(TTA)_{2,3}$-H21 were Reverse-Phase Cartridge•Gold^{TM} purified. Oligonucleotides were dissolved in bi-distilled water at a concentration of 200 μM and stored at −20°C. Concentrations were determined by UV absorption using molar extinction coefficients provided by the manufacturer.

UV absorption measurements

Oligonucleotides were dissolved in a 10 mM cacodylic acid buffer at pH 7.2 (adjusted with LiOH), containing 100 mM NaCl or KCl, at strand concentrations corresponding to 6 μM of potential G4 units (H21: 6 μM, H45: 3 μM, H69: 2 μM, H93: 1.5 μM, TTA-H45-TTA: 3 μM, H21-$(TTA)_{2,3}$-H21: 3 μM, H21-$(TTA)_{2,3}$-H21-$(TTA)_{2,3}$-H21: 2 μM). UV absorption measurements as a function of temperature (at 0.2°C min^{-1}), thermal difference spectra (TDS) and circular dichroism (CD) spectra (at 5°C) were acquired as previously described (37), using an Uvikon XL spectrophotometer (Secomam) and a J-810 spectropolarimeter (Jasco). Heating and cooling profiles were identical. We defined 'temperature of UV-thermal transition', $T_{1/2}{}^{UV}$, the intercept between the melting profile and the median line between low and high temperature baselines. For a two-state transition, $T_{1/2}{}^{UV}$ corresponds to the melting temperature T_m, defined as the temperature at which oligonucleotide unfolded and folded fractions are identical; for more complex thermal transition pathways, $T_{1/2}{}^{UV}$ is not necessarily identical to T_m.

Molecular-beacon assays

Fluorescence measurements were carried out on a SPEX Fluorolog spectrofluorimeter (Jobin Yvon) equipped with a circulating water bath to regulate the temperature of the cell holder. Aliquots of 0.208 μM molecular beacon MB solutions and of 20.8 μM H45 solutions were prepared in a 10 mM cacodylic acid buffer at pH 7.2 (adjusted with LiOH), containing 100 mM NaCl or KCl; the solutions were heated for 2 min at 90°C and slowly cooled at 4°C. For each experiment at a chosen temperature T, 500 μl of the 0.208 μM molecular beacon solution were put in a quartz cell and allowed to equilibrate at the temperature T in the spectrofluorimeter cell holder; the fluorescence emission of the molecular beacon solution was then recorded for 15 min.

Then, 20 μl of the 20.8 μM H45 solution, equilibrated at the temperature T in a water bath, were added and carefully mixed to the molecular beacon solution, and the fluorescence emission was recorded over time. Fluorescence emission was recorded at fixed wavelengths (specified in figure captions), upon excitation at 470 nm. Fluorescence emission intensities in the presence of H45 were corrected for dilution. Molecular-beacon assays were carried out with a highly pure H45 oligonucleotide (the presence of 10% truncated oligonucleotides folding into single G4s biases the assay).

Protein-binding assays

H45 oligonucleotide was labeled with [γ ^{32}P]ATP using a T4 polynucleotide kinase and purified by denaturing 15% polyacrylamide gel electrophoresis. Radiolabeled H45 was diluted at 2.5 nM strand concentration in a buffer containing 50 mM HEPES pH 7.9, 0.1 mg ml^{-1} bovin serum albumin (BSA), 100 mM KCl or NaCl and 2% glycerol, heated at 80°C for 5 min and slowly cooled at room temperature. Human Replication Protein A (hRPA) was diluted at various concentrations (25, 50, 125, 250 and 500 nM) in a buffer containing 50 mM Tris-HCl pH 7.5, 100 mM KCl, 1 mM dithiothreitol (DTT), 10% glycerol, 0.2 mg ml^{-1} BSA and 0.1 mM ethylenediaminetetraacetic acid (EDTA), and pre-incubated 20 min at 4°C. For electrophoretic mobility shift assay (EMSA) at a temperature T, 2 μl of hRPA solutions pre-incubated at T for 30 s were added to 8 μl of radiolabeled H45 solutions; H45/hRPA mixes were incubated for 20 min at T. Samples were then loaded on a 5% polyacrylamide gel (acrylamide:bisacrylamide 29:1) prepared in a 0.5X Tris-borate-EDTA (TBE) buffer containing 20 mM KCl or NaCl. Electrophoresis was carried out for 90 min at 7 V cm^{-1}, at the temperature T, in a 0.5X TBE buffer containing 20 mM KCl or NaCl. After electrophoresis, gels were dried and exposed on a Phosphorimager screen; screens were scanned with a Typhoon 9410 Imager (Molecular Dynamics). The intensities I of the bands were quantified using ImageQuant. For each hRPA concentration, the fraction of radiolabeled H45 bound to hRPA was calculated as $I_{\text{H45 bound to hRPA}} / (I_{\text{H45 bound to hRPA}} + I_{\text{free H45}})$.

Differential scanning calorimetry (DSC)

DSC measurements were carried out on a CSC 6100 Nano DSC II calorimeter (Calorimetry Sciences Corporation). H45 solutions at 100 μM strand concentration were prepared in a 10 mM cacodylic acid buffer at pH 7.2 (adjusted with LiOH), containing 100 mM NaCl or KCl. Oligonucleotides and buffer solutions were degassed prior to measurements. DSC thermograms were acquired in the 5–95°C temperature range, at a temperature scan rate of 0.5°C min^{-1} and at a constant pressure of 3 atm; three heating/cooling scans were collected; heating and cooling profiles were identical (opposite in sign). In order to verify that DSC profiles corresponded to states at thermodynamic equilibrium, DSC measurements were carried out at one additional temperature scan rate: thermograms were identical to the ones obtained at 0.5°C min^{-1}. DSC measurements were carried out twice using two independent H45 batches; thermograms were identical. Thermodynamic analyses were conducted using the CpCalc software. 'Buffer versus buffer' scans was subtracted from 'sample versus buffer' scans. Row microwatt data were converted to molar heat capacity C_p of the solute. The enthalpy change ΔH_{cal} upon folding was calculated as the area under the excess molar heat capacity function C_p^{excess} (obtained by subtracting to C_p a polynomial baseline fitting the pre- and post-transition regions of the DSC profile): $\Delta H_{cal} = \int C_p^{excess}(T)dT$. The entropy change ΔS_{cal} upon folding was calculated as $\Delta S_{cal} = \int (C_p^{excess}(T)/T)dT$.

RESULTS

The unusual case of (GGGTTA)$_7$GGG melting transition in sodium

We investigated by UV absorption spectroscopy, the structure and stability of (GGGTTA)$_{4m-1}$GGG telomeric sequences with $m = 1$, 2, 3 and 4 in sodium. These sequences are potentially able to fold into one, two, three and four contiguous G4 units, respectively. With regard to their length in nucleotides, we named these sequences H21 ($m = 1$), H45 ($m = 2$), H69 ($m = 3$) and H93 ($m = 4$). Similarly to what we reported in potassium (37), also in sodium H45, H69 and H93 folded into two, three and four contiguous G4 units, respectively (thermal difference spectra, circular dichroism spectra and gel electrophoresis migration patterns supporting folding into contiguous G4s are shown in Supplementary Figure S1). Similarly to what we observed in potassium (37), the UV-melting transitions of H21, H45, H69 and H93 structures in sodium shifted toward lower temperatures when increasing the number of G4 units composing them (Figure 1A). We provided an understanding of this behavior in terms of the stability of the single G4 units composing these tandem G4 structures in potassium (37). Unsurprisingly, the tandem G4 structures formed by H45, H69 and H93 in sodium had lower temperatures of UV-thermal transition ($T_{1/2}^{UV}$) than the structures formed in potassium (Table 1). Nevertheless, despite these expected behaviors, H45 displayed two unique and related features: (i) in sodium, the UV-melting transition of H45 (composed of two contiguous G4 units) was steeper than the ones of H21, H69 and H93 (composed of one, three and four G4 units, respectively) (Figure 1A); (ii) despite a lower $T_{1/2}^{UV}$, the H45 sodium structure displayed a steeper UV-melting transition than the H45 potassium structure (Figure 1B).

UV-melting profiles normalized between the minimum and the maximum of absorbance, as presented in Figure 1B, represent the folded fraction of G4 units as a function of temperature. They directly show that above about 45°C, the folded fraction of H45 G4 units in potassium is higher than in sodium. This means that, above this temperature, the G4 units composing H45 have a higher structural stability in potassium than in sodium. Nevertheless, analysis of H45 UV-melting transitions according to a simple two-state model suggests that folding of H45 in sodium may be driven by a more favorable enthalpy change than folding in potassium, and that the H45 sodium structure may become more stable than the potassium structure below a threshold temperature estimated to be around 45°C (Sup-

Table 1. Temperatures of UV-thermal transition of $(GGGTTA)_{4m-1}GGG$ oligonucleotide structures

sequence from 5′ to 3′	sequence name	number of G4 units	$T_{1/2}^{UV}$ (°C) NaCl	$T_{1/2}^{UV}$ (°C) KCl[1]
$(GGGTTA)_3GGG$	H21	1	58	68
$(GGGTTA)_7GGG$	H45	2	53	59
$(GGGTTA)_{11}GGG$	H69	3	45	56
$(GGGTTA)_{15}GGG$	H93	4	43	54

Temperatures of UV-thermal transition determined by absorbance at 295 nm of tandem G4 structures formed by $(GGGTTA)_{4m-1}GGG$ sequences (m = 1, 2, 3, 4) in the presence of 100 mM NaCl or KCl.
[1]Data reported in (37).

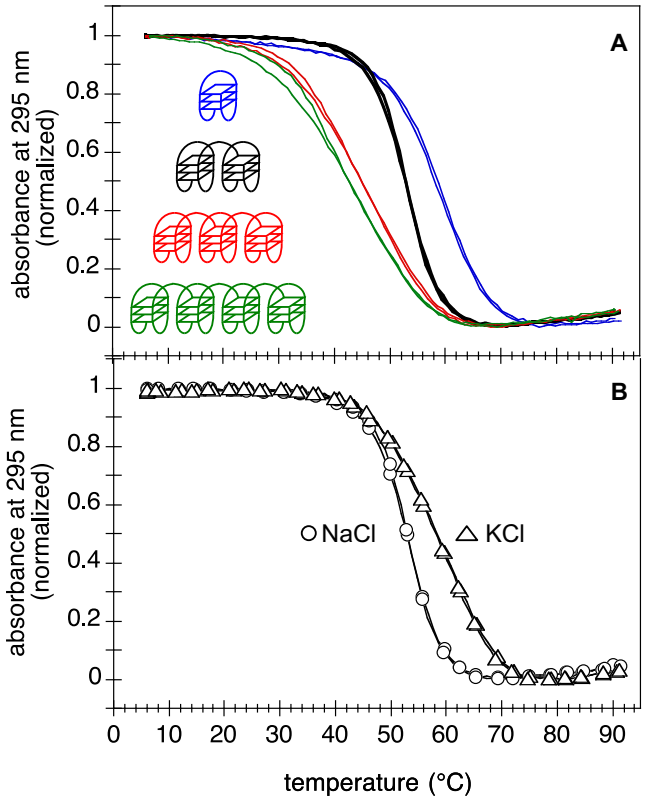

Figure 1. UV-melting profiles of $(GGGTTA)_{4m-1}GGG$ oligonucleotides. (**A**) Absorbance at 295 nm as a function of temperature of H21 (m = 1, blue line), H45 (m = 2, black bold line), H69 (m = 3, red line) and H93 (m = 4, green line) in 100 mM NaCl. (**B**) Absorbance at 295 nm as a function of temperature of H45 in 100 mM NaCl (circles) or KCl (triangles). Cooling and heating profiles are shown; they were normalized between the minimum and the maximum of absorbance. The conformation used to represent tandem G4s is speculative and for illustrative purpose.

plementary Figure S2). This conclusion, based on a model-dependent (and hence questionable) analysis of H45 UV-melting transitions, prompted us to experimentally investigate the relative stabilities and the energetics of H45 structures in sodium and in potassium using alternative methods.

Probing the relative stabilities of H45 structures in sodium and in potassium with a molecular beacon

In order to experimentally probe the relative stabilities of the structures formed by H45 in sodium and in potassium at temperatures below 45°C, we designed the following molecular beacon, named MB:

FAM-5′GATCTCAGG**TAACCCTAACCCTAAC CCCCTGAGATC**3′-Dabcyl.

This fluorescent oligonucleotide is composed of a loop of 18 bases (bold fonts) able to hybridize to the H45 sequence and of a stem of 9 base pairs (underlined fonts). A 6-carboxyfluorescein (FAM) and a Dabcyl quencher are covalently attached to its 5′ and 3′ extremities, respectively. When the molecular beacon is folded, the Dabcyl dye is in close proximity to the FAM dye and quenches FAM fluorescence; upon hybridization of the molecular beacon to H45, the FAM and the Dabcyl moieties move away from each other and the FAM fluorescence is restored. Thus, the increase of FAM emission in the presence of H45 allows monitoring the opening kinetics of the molecular beacon in the presence of H45.

As expected, the molecular beacon structure had identical melting profiles, hence identical stabilities, in sodium and in potassium (Supplementary Figure S3) (the stability and kinetic parameters of DNA duplexes or hairpins are independent of the nature of the monovalent cation, Na^+ or K^+, present in solution). Hence, differences in the opening kinetics of the molecular beacon in sodium and in potassium directly reflect differences in the stability of the H45 sodium and potassium structures. We recorded the fluorescence emission of the molecular beacon in the presence of H45 over time at different temperatures. At 45°C, the opening kinetics of the molecular beacon in the presence of H45 in sodium and in potassium were almost identical (Figure 2A). At lower temperatures, the opening kinetics of the molecular beacon to H45 in sodium was significantly slower than in potassium (Figure 2B at 35°C; Supplementary Figure S4 at 37°C and at 30°C). These results directly demonstrate that, at 45°C, the structures of H45 in sodium and in potassium have similar stabilities, while, at lower temperatures, the structure formed by H45 in sodium is more stable than the structure formed in potassium.

Altogether, UV-melting profiles and molecular-beacon assays directly reveal that at about 45°C there is a switch in the relative stability of the H45 sodium and potassium structures.

Interestingly, this unusual behavior was affected by the presence of 5′ and 3′ flanking tails. TTA-$(GGGTTA)_7GGG$-TTA oligonucleotide, named TTA-H45-TTA, did not exhibit the peculiar behavior of H45: the UV-melting transition of TTA-H45-TTA in sodium was not steeper than its UV-melting transition in potassium, and its sodium conformation was less stable than its potassium counterpart at all temperatures (Supplementary Figure S5). Hence, a higher stability in sodium than in

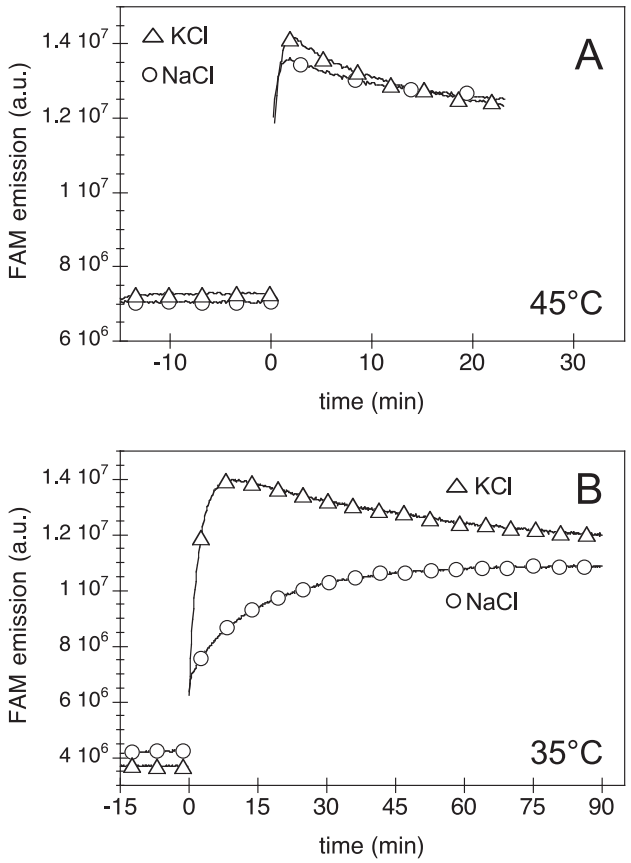

Figure 2. Opening kinetics of the molecular beacon in the presence of H45. Fluorescence emission of 0.2 μM molecular beacon MB alone ($t < 0$) and in the presence of 0.8 μM H45 ($t > 0$), in 100 mM NaCl (circles) or KCl (triangles), at 45°C (**A**) and at 35°C (**B**). Excitation wavelength: 470 nm; emission wavelength: 520 nm. The fluorescence intensity of the molecular beacon alone ($t < 0$) depends on the temperature (about 7×10^6 a.u. at 45°C and about 4×10^6 a.u. at 35°C); this is because the FAM emission of the molecular beacon is proportional to the molecular beacon unfolded fraction, which increases with the temperature (Supplementary Figure S4).

potassium is not a general feature of telomeric structures composed of two contiguous G4 units; it is a unique feature of the H45 structure, lacking flanking tails.

Probing the relative stabilities of H45 structures in sodium and in potassium with a protein-binding assay

To provide additional experimental evidence that H45 forms a more stable structure in sodium than in potassium below 45°C, we carried out a protein-binding assay. Replication Protein A (RPA) is a single-stranded DNA binding protein. In a previous work, we proved that there is a clear inverse relationship between its binding affinity to a G4-prone DNA sequence and the stability of the formed G4 structure; in particular, hRPA bound and unwound the single telomeric G4 formed by the $(GGGTTA)_3GGG$ sequence more efficiently in sodium than in potassium (38).

We slowly annealed radiolabeled H45 in sodium or in potassium, then we added increasing concentrations of hRPA; after incubation at 37°C, we carried out an electrophoretic mobility shift assay at the same temperature to evaluate the percentage of radiolabeled H45 bound to hRPA as a function of hRPA concentration. Figure 3A shows the migration patterns of radiolabeled H45 in the presence of hRPA; the two retarded bands correspond to hRPA:H45 1:1 and 2:1 complexes (39). In agreement with a higher stability in sodium, the percentage of H45 bound to hRPA was significantly lower in sodium than in potassium (Figure 3B). The same trend was observed at lower temperatures (30°C and 20°C, Supplementary Figure S6). This result provides further evidence that, at temperatures where H45 is completely folded (i.e. below about 45°C), the structure formed by H45 in sodium is more stable than the structure formed in potassium.

We then investigated the thermodynamic reasons underlying the switch in the relative stability of the H45 sodium and potassium structures.

Measurement of enthalpy changes upon H45 folding with DSC

The steepness of H45 UV-melting transition in sodium suggests that the switch in sodium/potassium relative stability occurring around 45°C may arises from a greater favorable enthalpy change upon folding in sodium. In order to evaluate enthalpy changes upon H45 folding with a model-independent approach, we carried out DSC experiments (40).

In agreement with UV-melting transitions, the DSC profile of H45 in sodium was shifted toward lower temperatures compared to H45 in potassium (Figure 4 and Table 2). Importantly, DSC directly demonstrated that folding of H45 in sodium resulted in a greater favorable enthalpy change than folding in potassium (Figure 4 and Table 2). Notably, the DSC peaks in sodium and in potassium had different shapes. The DSC peak of H45 in potassium was asymmetric and broad (Full Width at Half Maximum of about 20°C), as previously observed for other telomeric tandem G4s in potassium (36). In a previous work, we showed that the two G4 units composing the H45 structure in potassium have different stabilities and do not interact with each other, which may explain the asymmetry and broadness of the DSC peak of H45 in potassium. The DSC peak of H45 in sodium was symmetric and actually narrower than DSC peaks of single telomeric G4s: its Full Width at Half Maximum was about 10°C, while it varies from 15°C to about 25°C for single telomeric G4s, depending on the nucleotides flanking the $(GGGTTA)_3GGG$ core sequence (36,41–44). This suggests that, in contrast to the potassium structure, the H45 sodium structure behaves as a single structural entity and not as two independent G4 units.

We then investigated the nature of the molecular interactions underlying the enthalpy driven stabilization of the H45 sodium structure.

Probing interactions between G4 units in sodium structures

We investigated if the two G4 units composing the H45 sodium structure interacted with each other. To this purpose, we studied H21-$(TTA)_{n=1,2,3}$-H21 sequences, where H21 is the 21mer sequence $(GGGTTA)_3GGG$. These sequences fold into two contiguous G4 units separated by

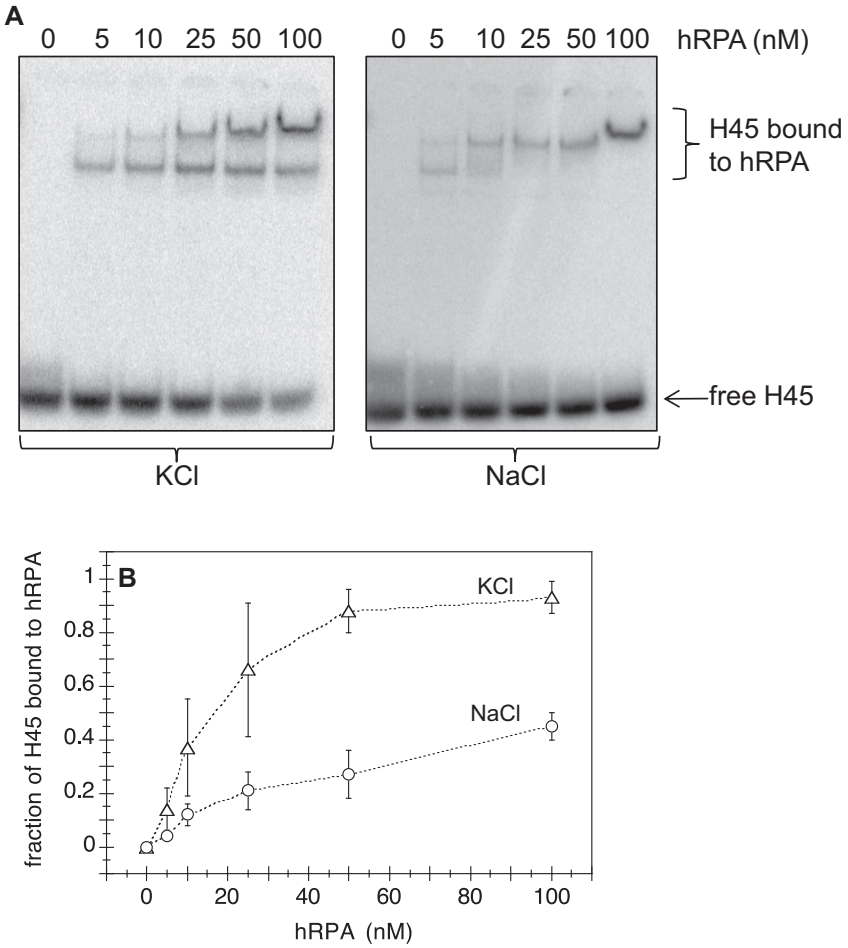

Figure 3. Binding of hRPA to H45. (**A**) Migration patterns of 2 nM radiolabeled H45 in KCl or NaCl incubated at 37°C in the presence of increasing concentrations of hRPA. Electrophoresis was carried out at 37°C, in polyacrylamide gels and migration buffers supplemented with 20 mM KCl or NaCl. (**B**) Fraction of radiolabeled H45 bound to hRPA as a function of hRPA concentration, in NaCl (circles) or KCl (triangles), at 37°C. Radiolabeled H45 bound fractions are average values obtained from analysis of three independent experiments.

one ($n = 1$), two ($n = 2$) or three ($n = 3$) TTA repeats (for $n = 1$, the sequence is H45). In potassium, the structures formed by these three sequences had identical UV-melting profiles (Figure 5A), as previously reported (37). Conversely, in sodium, the temperature of UV-thermal transition $T_{1/2}{}^{UV}$ and the steepness of the transition decreased with increasing the number n of TTA repeats separating the two G4 units (Figure 5B). These results support that, while the two G4 units composing the H45 structure behave independently in potassium conditions, they favorably interact with each other in sodium. This stabilizing interaction in sodium is impaired upon increasing the number n of TTA repeats separating the two G4 units; for $n = 2$, the structure formed in sodium is less stable than the structure formed in potassium at all temperatures (Supplementary Figure S9). This positive cooperativity between adjacent G4 units was only observed for H45. The normalized UV-melting profiles of the structures formed by H21-$(TTA)_n$-H21-$(TTA)_n$-H21 sequences, folding into three contiguous G4 units, were independent of the length of the $(TTA)_{n\,=\,1,2,3}$ linker (Figure 5C). Hence, the presence of a third G4 unit impairs the stabilizing interaction between two contiguous G4 units revealed in the H45 sodium structure.

DISCUSSION

Nearly 50 years ago, Chantot and Guschlbauer reported 'interestingly enough there is a large difference between the melting points measured in KCl and those measured in NaCl solutions' for 8-bromoguanosine gels (4). Since then many studies on a variety of G4-prone nucleic acid sequences have shown that potassium conformations are generally more stable than sodium conformations. This differential Na^+/K^+ sensitivity is often considered a fingerprint of G4 formation, other nucleic acid structures being independent of the nature of the monovalent cation. For example, Chambers *et al.* took advantage of this differential Na^+/K^+ sensitivity to develop a sequencing-based method to detect G4s genome-wide (45). In this article we report the first example of a higher-order G4 motif whose sodium conformation is more stable than its potassium conformation.

While studying the reasons underlying the complex melting behaviors of long telomeric DNA sequences able to fold into contiguous G4 units, we realized that the

Table 2. DSC measurements

	T_{max}^{DSC} (°C)	FWHM (°C)	ΔH_{cal} kcal mol^{-1}	ΔS_{cal} kcal mol^{-1} K^{-1}
NaCl	55 ± 1	10 ± 1	−80 ± 4	−0.243 ± 0.010
KCl	63 ± 1	19 ± 2	−68 ± 3	−0.202 ± 0.010

Results from analysis of DSC scans on 100 μM H45 in 100 mM NaCl or KCl. T_{max}^{DSC} is the temperature of maximal heat uptake or release. FWHM is the full width at half maximum of the DSC peaks. ΔH_{cal} and ΔS_{cal} are the enthalpy and entropy changes upon folding.

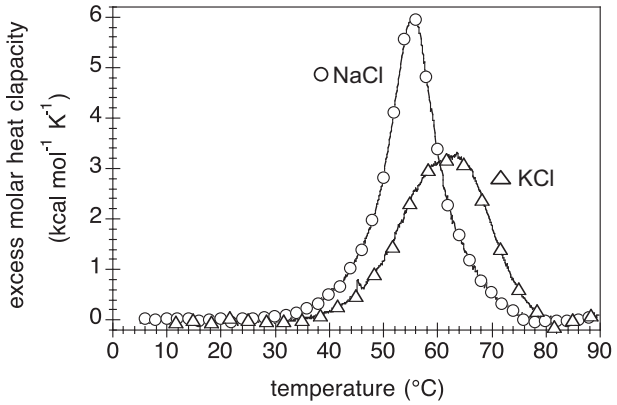

Figure 4. DSC profiles of H45. Excess molar heat capacity as a function of temperature of 100 μM H45, upon heating at 0.5°C min^{-1}, in 100 mM NaCl (circles) or KCl (triangles). Molar heat capacities and polynomial baselines are shown in Supplementary Information (Supplementary Figure S7). In order to verify that DSC profiles corresponded to states at thermodynamic equilibrium, DSC measurements were carried out at one additional temperature scan rate: thermograms were identical to the ones obtained at 0.5°C min^{-1} (Supplementary Figure S8).

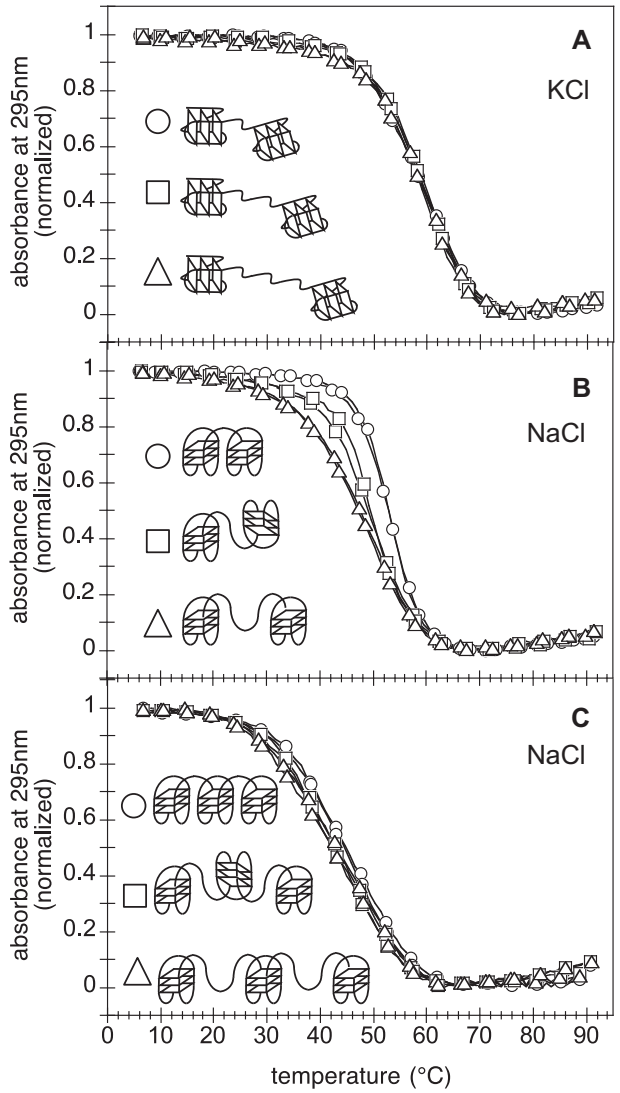

Figure 5. UV-melting profiles of H21-(TTA)$_n$-H21 and H21-(TTA)$_n$-H21-(TTA)$_n$-H21 oligonucleotides. (**A**,**B**) Absorbance at 295 nm as a function of temperature of H21-(TTA)$_n$-H21 (circles: $n = 1$; squares: $n = 2$; triangles: $n = 3$) in 100 mM KCl (A) or NaCl (B) (for $n = 1$, the sequence is H45). (**C**) Absorbance at 295 nm as a function of temperature of H21-(TTA)$_n$-H21-(TTA)$_n$-H21 (circles: $n = 1$; squares: $n = 2$; triangles: $n = 3$) in 100 mM NaCl (for $n = 1$, the sequence is H69). Cooling and heating profiles are shown; they were normalized between the minimum and maximum of absorbance. The conformations used to represent tandem G4s are speculative and for illustrative purpose.

(GGGTTA)$_7$GGG sequence (H45), folding into two contiguous G4 units, displayed in sodium an UV-melting transition uncommonly steep. This feature attracted our attention and prompted us to a deeper investigation. Three independent approaches (UV-melting, molecular beacon, protein-binding assay) allowed us to conclude that the (GGGTTA)$_7$GGG sodium and potassium conformations display a switch in their relative stability. On one hand, UV-melting experiments reveled that above 45°C the potassium conformation is more stable than the sodium conformation; on the other hand, isothermal molecular-beacon and protein-binding assays provided direct evidence that below 45°C the sodium conformation is more stable than the potassium conformation. DSC measurements and the study of G4 units separated by (TTA)$_n$ linkers of increasing length allowed revealing the thermodynamic and molecular reasons underlying this switch in the potassium/sodium (GGGTTA)$_7$GGG relative stability: folding in sodium is driven by a more favorable enthalpy change, resulting from stabilizing interactions between the two G4 units. Conversely, in spite of predictions based on molecular dynamics simulations (46,47), there is no experimental evidence of stabilizing interactions between G4 units in telomeric tandem G4s in potassium solutions, in particular for the (GGGTTA)$_7$GGG potassium structure (36,37).

Overall, our work allows drawing the following schematic picture of the relative stabilities of (GGGTTA)$_7$GGG sodium and potassium structures along their folding pathways. G4 units in potassium fold at higher temperatures than G4 units in sodium, as directly showed by melting profiles; this means that the two G4 units are individually more stable in potassium than in sodium. Nevertheless, while in potassium the two G4 units do not interact with each other,

in sodium, once both of them are folded, they interact with each other. This interaction makes the $(GGGTTA)_7GGG$ structure in sodium more stable than the structure in potassium. Ultimately, the switch in the relative stability of the sodium and potassium structures of the $(GGGTTA)_7GGG$ sequence results from the interplay between 'G4 cation-dependent stability' and 'G4 cation-dependent conformation': potassium ions drive folding of its individual G4 units into more stable conformation(s) than sodium; sodium ions drive folding of its individual G4 units into conformation(s) allowing the establishment of stabilizing interactions between them.

Structural studies on $(GGGTTA)_7GGG$ in sodium will be necessary to gain insight into the conformation(s) and the spatial arrangement of the two G4 units and to reveal, at atomic level, the nature of the interactions between them. Our results show that $(GGGTTA)_7GGG$ in sodium behaves as a single structural entity. We propose a speculative schematic model of the conformation and spatial arrangement of the two interacting G4 units in the $(GGGTTA)_7GGG$ sodium structure. CD spectra and a structural investigation on individually labeled G4 units suggest that telomeric tandem G4s in sodium fold into an antiparallel conformation (48). We speculate that the two G4 units in the $(GGGTTA)_7GGG$ sodium structure might be in antiparallel conformations and aligned one on top of the other, so that the 5′ and 3′ extremities are at the interface of the two G4 units. The presence of third G4 units or of TTA tails would be a factor of steric hindrance impairing this speculative spatial arrangement prone to interactions between two contiguous G4 units (antiparallel conformations allow the alignment along the G4 cavity axis of only two G4 units; a third G4 unit will necessary be out of axis).

We cannot rule out the existence of a fraction of H45 sodium structures where the two G4 units do not interact with each other (because of structural polymorphism) or the existence of a fraction of folding intermediates. Nevertheless, if a fraction of H45 sodium structures less stable than H45 potassium structures exists, this fraction constitutes a minor fraction (<0.1) of the H45 sodium population. This is supported by results obtained with the molecular-beacon assay. Indeed, while the protein-binding assay in Figure 3 reflects the stability of the whole H45 population (protein concentration exceeded H45 concentration), the molecular-beacon assay in Figure 2 reflects the stability of the less stable 0.1 fraction of the whole population (the MB concentration was one-tenth of the H45 concentration).

The unusual behavior displayed by the $(GGGTTA)_7GGG$ telomeric sequence has practical implications for the design of telomeric ligands and the understanding of higher-order G4 structures in genomes. Stabilization of G4 structures at telomeres with small ligands is a potential strategy to interfere with human tumor cell proliferation (49). Since telomeric G4s likely come in tandem, there is rising interest in designing small ligands able to bind tandem G4s. Such ligands may allow selectively targeting telomeric tandem G4s over isolated G4s spread in other regions of the genome. In light of our results, it seems not judicious to use the $(GGGTTA)_7GGG$ sequence and sodium solutions for *in vitro* characterization of ligands designed to bind to telomeric tandem G4s in cells. Likely, the $(GGGTTA)_7GGG$ sodium structure, with its peculiar behavior, is not a suitable model for tandem G4s at telomeres. This might explain why ligands selectively binding to this structure do not interact with telomeres in human cells (50,51).

Higher-order G4 structures can also potentially form in genomic regions other than telomeres and may be involved in genome regulation (52,53). Expansions of G4 motifs are associated with neurological diseases (54). We are scanning various G4-prone sequences to check if this potassium/sodium stability switch is unique to the human telomeric $(GGGTTA)_7GGG$ sequence or is shared with other higher-order G4 motifs. Higher-order G4 motifs displaying a higher structural stability in sodium than in potassium might play a role of functional switches turned on by transiently high local Na^+ concentrations. It might be that, for such higher-order G4 motifs, the structures induced by K^+ physiological concentrations are efficiently unwound by appropriate proteins, and that only a transiently high local concentration of Na^+ induces folding into structures sufficiently stable to carry out a regulatory function at the right time. Interestingly, our protein-binding assay showed that hRPA was able to efficiently bind, and likely unwind (38), the $(GGGTTA)_7GGG$ potassium structure but not the sodium structure.

In conclusion, we provided the first example of a higher-order G4 structure more stable in sodium than in potassium. Usually, the relative stability of G4 structures is inappropriately assessed by simply comparing thermal transition temperatures values. Here, we provided a sound demonstration that, despite a lower thermal stability (i.e. lower $T_{1/2}{}^{UV}$ and $T_{max}{}^{DSC}$), the sodium structure of the $(GGGTTA)_7GGG$ sequence is more stable than the potassium structure at temperatures at which it is completely folded (i.e. below 45°C, where the folded fraction is nearly 1). Compared to single G4s, higher-order G4 structures formed by more than one structural domain have a supplementary level of possible intramolecular interactions, the one between distinct structural domains. Our findings on $(GGGTTA)_7GGG$ sequence demonstrate that stabilizing interactions between G4 structural domains can make a higher-order structure in sodium more stable than its counterparts in potassium, even though its single G4 structural domains are more stable in potassium than in sodium. In this sense, the $(GGGTTA)_7GGG$ sequence is the exception that confirms the $K^+ > Na^+$ general trend for G4 stabilization. It seems that, despite many years of investigation, G4 structures still reserve unexpected behaviors.

SUPPLEMENTARY DATA

Supplementary Data are available at NAR Online.

ACKNOWLEDGEMENTS

We thank Dr Emmanuelle Delagoutte for her contribution in RPA production and purification. We thank the members of the team 'Nucleic Acid Structures, Telomeres and Evolution' for helpful discussions.

FUNDING

Muséum National d'Histoire Naturelle (MNHN); Centre National de la Recherche Scientifique (CNRS); Institut National de la Santé et de la Recherche Médicale (INSERM). Funding for open access charge: Institut National de la Santé et de la Recherche Médicale (INSERM).
Conflict of interest statement. None declared.

REFERENCES

1. Gellert,M., Lipsett,M.N. and Davies,D.R. (1962) Helix formation by guanylic acid. *Proc. Natl. Acad. Sci. U.S.A.*, **48**, 2013–2018.
2. Williamson,J.R., Raghuraman,M.K. and Cech,T.R. (1989) Monovalent cation-induced structure of telomeric DNA: the G-quartet model. *Cell*, **59**, 871–880.
3. Rich,A. (1958) The molecular structure of polyinosinic acid. *Biochim. Biophys. Acta*, **29**, 502–509.
4. Chantot,J. and Guschlbauer,W. (1969) Physicochemical properties of nucleosides 3. Gel formation by 8-bromoguanosine. *FEBS Lett.*, **4**, 173–176.
5. Pinnavaia,T.J., Marshall,C.L., Mettler,C.M., Fisk,C.L., Miles,H.T. and Becker,E.D. (1978) Alkali metal ion specificity in the solution ordering of a nucleotide, 5′-guanosine monophosphate. *J. Am. Chem. Soc.*, **100**, 3625–3627.
6. Miles,H.T. and Frazier,J. (1978) Infrared spectroscopy of polynucleotides in the carbonyl region in H2O solution: A.U Systems. *Biochemistry*, **17**, 2920–2927.
7. Kang,C., Zhang,X., Ratliff,R., Moyzis,R. and Rich,A. (1992) Crystal structure of four-stranded Oxytricha telomeric DNA. *Nature*, **356**, 126–131.
8. Laughlan,G., Murchie,A.I., Norman,D.G., Moore,M.H., Moody,P.C., Lilley,D.M. and Luisi,B. (1994) The high-resolution crystal structure of a parallel-stranded guanine tetraplex. *Science*, **265**, 520–524.
9. Hardin,C.C., Watson,T., Corregan,M. and Bailey,C. (1992) Cation-dependent transition between the quadruplex and Watson-Crick hairpin forms of d(CGCG3GCG). *Biochemistry*, **31**, 833–841.
10. Hud,N.V., Smith,F.W., Anet,F.A. and Feigon,J. (1996) The selectivity for K +versus Na+ in DNA quadruplexes is dominated by relative free energies of hydration: a thermodynamic analysis by 1H NMR. *Biochemistry*, **35**, 15383–15390.
11. Mergny,J.L., Gros,J., De Cian,A., Bourdoncle,A., Rosu,F., Saccà,B., Guittat,L., Amrane,S., Mills,M. and Alberti,P. (2006) In: Neidle,S. and Balasubramanian,S. *et al.* (eds.), *Quadruplex Nucleic Acids*. RSC Publishing, Cambridge, pp. 31–80.
12. Hud,N.V. and Plavec,J. (2006) In: Neidle,S. and Balasubramanian,S. (eds), *Quadruplex Nucleic Acids*. RSC Publishing, Combridge, pp. 100–130.
13. Mergny,J.L., Phan,A.T. and Lacroix,L. (1998) Following G-quartet formation by UV-spectroscopy. *FEBS Lett.*, **435**, 74–78.
14. Dominick,P.K. and Jarstfer,M.B. (2004) A conformationally constrained nucleotide analogue controls the folding topology of a DNA g-quadruplex. *J. Am. Chem. Soc.*, **126**, 5050–5051.
15. Risitano,A. and Fox,K.R. (2004) Influence of loop size on the stability of intramolecular DNA quadruplexes. *Nucleic Acids Res.*, **32**, 2598–2606.
16. Sacca,B., Lacroix,L. and Mergny,J.L. (2005) The effect of chemical modifications on the thermal stability of different G-quadruplex-forming oligonucleotides. *Nucleic Acids Res.*, **33**, 1182–1192.
17. Risitano,A. and Fox,K.R. (2005) Inosine substitutions demonstrate that intramolecular DNA quadruplexes adopt different conformations in the presence of sodium and potassium. *Bioorg. Med. Chem. Lett.*, **15**, 2047–2050.
18. Gros,J., Rosu,F., Amrane,S., De Cian,A., Gabelica,V., Lacroix,L. and Mergny,J.L. (2007) Guanines are a quartet's best friend: impact of base substitutions on the kinetics and stability of tetramolecular quadruplexes. *Nucleic Acids Res.*, **35**, 3064–3075.
19. Gros,J., Avino,A., Lopez de la Osa,J., Gonzalez,C., Lacroix,L., Perez,A., Orozco,M., Eritja,R. and Mergny,J.L. (2008) 8-Amino guanine accelerates tetramolecular G-quadruplex formation. *Chem. Commun.*, **25**, 2926–2928.
20. Guedin,A., De Cian,A., Gros,J., Lacroix,L. and Mergny,J.L. (2008) Sequence effects in single-base loops for quadruplexes. *Biochimie*, **90**, 686–696.
21. De Cian,A., Grellier,P., Mouray,E., Depoix,D., Bertrand,H., Monchaud,D., Teulade-Fichou,M.P., Mergny,J.L. and Alberti,P. (2008) Plasmodium telomeric sequences: structure, stability and quadruplex targeting by small compounds. *Chembiochem*, **9**, 2730–2739.
22. Gros,J., Guedin,A., Mergny,J.L. and Lacroix,L. (2008) G-Quadruplex formation interferes with P1 helix formation in the RNA component of telomerase hTERC. *Chembiochem*, **9**, 2075–2079.
23. Guedin,A., Alberti,P. and Mergny,J.L. (2009) Stability of intramolecular quadruplexes: sequence effects in the central loop. *Nucleic Acids Res.*, **37**, 5559–5567.
24. Tomasko,M., Vorlickova,M. and Sagi,J. (2009) Substitution of adenine for guanine in the quadruplex-forming human telomere DNA sequence G(3)(T(2)AG(3))(3). *Biochimie*, **91**, 171–179.
25. Guedin,A., Gros,J., Alberti,P. and Mergny,J.L. (2010) How long is too long? Effects of loop size on G-quadruplex stability. *Nucleic Acids Res.*, **38**, 7858–7868.
26. Tran,P.L., Mergny,J.L. and Alberti,P. (2011) Stability of telomeric G-quadruplexes. *Nucleic Acids Res.*, **39**, 3282–3294.
27. Dumas,A. and Luedtke,N.W. (2011) Highly fluorescent guanosine mimics for folding and energy transfer studies. *Nucleic Acids Res.*, **39**, 6825–6834.
28. Aggrawal,M., Joo,H., Liu,W., Tsai,J. and Xue,L. (2012) 8-Oxo-7,8-dihydrodeoxyadenosine: the first example of a native DNA lesion that stabilizes human telomeric G-quadruplex DNA. *Biochem. Biophys. Res. Commun.*, **421**, 671–677.
29. Marusic,M. and Plavec,J. (2015) The effect of DNA sequence directionality on G-Quadruplex folding. *Angew. Chem. Int. Ed. Engl.*, **54**, 11716–11719.
30. Ohtsuka,K., Sato,S., Sato,Y., Sota,K., Ohzawa,S., Matsuda,T., Takemoto,K., Takamune,N., Juskowiak,B., Nagai,T. *et al.* (2012) Fluorescence imaging of potassium ions in living cells using a fluorescent probe based on a thrombin binding aptamer-peptide conjugate. *Chem. Commun.*, **48**, 4740–4742.
31. Mekmaysy,C.S., Petraccone,L., Garbett,N.C., Ragazzon,P.A., Gray,R., Trent,J.O. and Chaires,J.B. (2008) Effect of O6-methylguanine on the stability of G-quadruplex DNA. *J. Am. Chem. Soc.*, **130**, 6710–6711.
32. Skolakova,P., Bednarova,K., Vorlickova,M. and Sagi,J. (2010) Quadruplexes of human telomere dG(3)(TTAG(3))(3) sequences containing guanine abasic sites. *Biochem. Biophys. Res. Commun.*, **399**, 203–208.
33. Sagi,J., Renciuk,D., Tomasko,M. and Vorlickova,M. (2010) Quadruplexes of human telomere DNA analogs designed to contain G:A:G:A, G:G:A:A, and A:A:A:A tetrads. *Biopolymers*, **93**, 880–886.
34. Yu,H.Q., Miyoshi,D. and Sugimoto,N. (2006) Characterization of structure and stability of long telomeric DNA G-quadruplexes. *J. Am. Chem. Soc.*, **128**, 15461–15468.
35. Xu,Y., Ishizuka,T., Kurabayashi,K. and Komiyama,M. (2009) Consecutive formation of G-quadruplexes in human telomeric-overhang DNA: a protective capping structure for telomere ends. *Angew. Chem. Int. Ed. Engl.*, **48**, 7833–7836.
36. Petraccone,L., Spink,C., Trent,J.O., Garbett,N.C., Mekmaysy,C.S., Giancola,C. and Chaires,J.B. (2011) Structure and stability of higher-order human telomeric quadruplexes. *J. Am. Chem. Soc.*, **133**, 20951–20961.
37. Bugaut,A. and Alberti,P. (2015) Understanding the stability of DNA G-quadruplex units in long human telomeric strands. *Biochimie*, **113**, 125–133.
38. Safa,L., Delagoutte,E., Petruseva,I., Alberti,P., Lavrik,O., Riou,J.F. and Saintome,C. (2014) Binding polarity of RPA to telomeric sequences and influence of G-quadruplex stability. *Biochimie*, **103**, 80–88.
39. Salas,T.R., Petruseva,I., Lavrik,O., Bourdoncle,A., Mergny,J.L., Favre,A. and Saintome,C. (2006) Human replication protein A unfolds telomeric G-quadruplexes. *Nucleic Acids Res.*, **34**, 4857–4865.
40. Pagano,B., Randazzo,A., Fotticchia,I., Novellino,E., Petraccone,L. and Giancola,C. (2013) Differential scanning calorimetry to investigate G-quadruplexes structural stability. *Methods*, **64**, 43–51.

41. Antonacci,C., Chaires,J.B. and Sheardy,R.D. (2007) Biophysical characterization of the human telomeric (TTAGGG)4 repeat in a potassium solution. *Biochemistry*, **46**, 4654–4660.
42. Gray,R.D., Li,J. and Chaires,J.B. (2009) Energetics and kinetics of a conformational switch in G-quadruplex DNA. *J. Phys. Chem. B*, **113**, 2676–2683.
43. Boncina,M., Lah,J., Prislan,I. and Vesnaver,G. (2012) Energetic basis of human telomeric DNA folding into G-quadruplex structures. *J. Am. Chem. Soc.*, **134**, 9657–9663.
44. Hayden,K.L. and Graves,D.E. (2014) Addition of bases to the 5′-end of human telomeric DNA: influences on thermal stability and energetics of unfolding. *Molecules*, **19**, 2286–2298.
45. Chambers,V.S., Marsico,G., Boutell,J.M., Di Antonio,M., Smith,G.P. and Balasubramanian,S. (2015) High-throughput sequencing of DNA G-quadruplex structures in the human genome. *Nat. Biotechnol.*, **33**, 877–881.
46. Haider,S., Parkinson,G.N. and Neidle,S. (2008) Molecular dynamics and principal components analysis of human telomeric quadruplex multimers. *Biophys. J.*, **95**, 296–311.
47. Petraccone,L., Trent,J.O. and Chaires,J.B. (2008) The tail of the telomere. *J. Am. Chem. Soc.*, **130**, 16530–16532.
48. Singh,V., Azarkh,M., Drescher,M. and Hartig,J.S. (2012) Conformations of individual quadruplex units studied in the context of extended human telomeric DNA. *Chem. Commun.*, **48**, 8258–8260.
49. Neidle,S. (2010) Human telomeric G-quadruplex: the current status of telomeric G-quadruplexes as therapeutic targets in human cancer. *FEBS J.*, **277**, 1118–1125.
50. Zhao,C., Wu,L., Ren,J., Xu,Y. and Qu,X. (2013) Targeting human telomeric higher-order DNA: dimeric G-quadruplex units serve as preferred binding site. *J. Am. Chem. Soc.*, **135**, 18786–18789.
51. Wang,J., Chen,Y., Ren,J., Zhao,C. and Qu,X. (2014) G-Quadruplex binding enantiomers show chiral selective interactions with human telomere. *Nucleic Acids Res.*, **42**, 3792–3802.
52. Petraccone,L. (2013) Higher-order quadruplex structures. *Top. Curr. Chem.*, **330**, 23–46.
53. Maizels,N. and Gray,L.T. (2013) The G4 genome. *PLoS Genet.*, **9**, e1003468.
54. Maizels,N. (2015) G4-associated human diseases. *EMBO Rep.*, **16**, 910–922.